JOURNAL OF OPTOELECTRONICS AND ADVANCED MATERIALS Vol. 8, No. 1, February 2006, p. 372 - 375

Numerical investigations of interstitial hole-assistant microstructured optical fiber

X. YU*, P. SHUM, M. TANG, M. YAN, J. LOVE[a]
Network Technology Research Centre, Nanyang Technological University, 50 Nanyang Drive, Research TechnoPlaza, 4th Storey, Singapore 637553
[a]*Research School of Physical Sciences & Engineering& Department of Physics, Australian National University, Australia*

We evaluate numerically the optical characteristics of a new type of microstructured optical fiber with interstitial air holes (IH-MOF). By modification of the basic hexagonal unit cell, different optical waveguide properties can be achieved. Endlessly single mode operation is obtainable from these IH-MOF structures with smaller air-hole diameter to pitch ratio (**d/Λ**<0.25) compared with conventional triangular-latticed MOFs. The zero-dispersion-wavelength is blue-shifted with the increase of interstitial air-hole size. Leaky loss and effective mode area is significantly reduced thus the nonlinearity is enhanced by a tighter confinement.

(Received November 5, 2005; accepted January 26, 2006)

Keyword: Photonic crystal fiber, Microstructured optical fiber, Cutoff, Chromatic dispersion, Confinement loss, Nonlinearity

1. Introduction

Photonic crystal fibers (PCFs) have attracted many attentions from research groups all over the world in recent ten years. There are two kinds of guiding mechanisms for PCF, one is due to the average index difference between the silica core and the periodic holey cladding, and the guiding basis is the same as the total internal reflection mechanism in conventional optical fibers. This group of PCFs is usually referred as microstructured optical fiber (MOF). They are fascinating because of various novel properties, such as endlessly single-mode operation [1], scalable dispersion [2] and nonlinearity [3], etc. The second group guide light using the photonic bandgap (PBG) effects [4], where light is confined in the hollow core due to the Bragg reflection of the periodic cladding. J. Broeng *et al*. has proposed a PBG structure with interstitial holes in order to increase the bandgap size [5]. This work was initiated by the interest in the observations of tiny interstitial air holes remaining in the fiber cladding after drawing. This structure is proven to be readily fabricated. Similar structures can be easily obtained during the stack and drawing fabrication process in index-guiding MOFs. Interstitial holes are also located among the gaps of capillaries as shown in Fig. 1 (a). However, so far the optical characteristics of such interstitial hole-assistant MOF (IH-MOF) structures have not been investigated yet. In this paper, we explored the optical properties of such IH-MOFs including modal cutoff condition, chromatic dispersion and mode confinement.

The defining parameters of the structure in Fig. 1(c) are the physical pitch (distance between the neighboring air holes) **Λ**, the diameter of the air hole centred in the unit cell **d**, and the diameter of the interstitial air hole **p**. We use a value of **n**=1.45 for fused silica throughout the calculations. Among various numerical modeling, full-vector finite element method (FEM) is proven to be the most accurate method. However for the complex holey structure in MOF, the number of mesh will be dramatically large and the computational efficiency is rather low [6]. Here we use the semi-vector beam propagation method (BPM), which is proven to be more straightforward and efficient. The parameters used in the BPM are as follows: the step size in longitudinal direction is 0.1μm, the number of grid points along transversal directions are both 260 with a transparent boundary condition. A correlation mode solver is used. The calculated results of the effective cladding index are shown in Fig. 2, and the discrepancy between BPM and FEM is rather small for a large wavelength range.

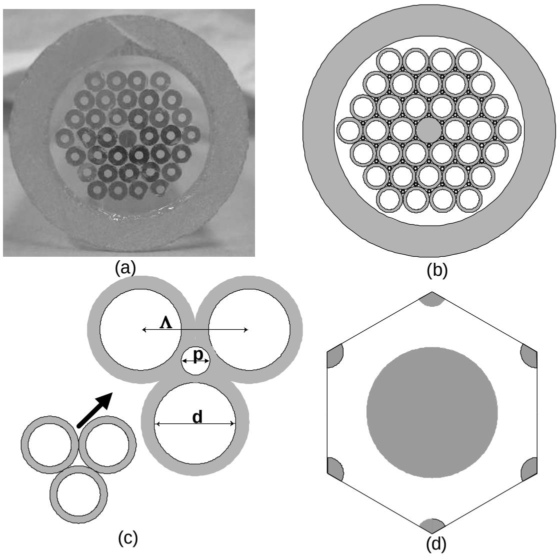

*Fig. 1. (a) Stack of capillaries for normal triangular latticed MOF preform (b) MOF preform with interstitial capillaries (c) IH-MOF design: **Λ**-pitch size, **d**-air hole diameter, **p**-interstitial hole diameter (d) hexagonal unit cell for the IH-MOF.*

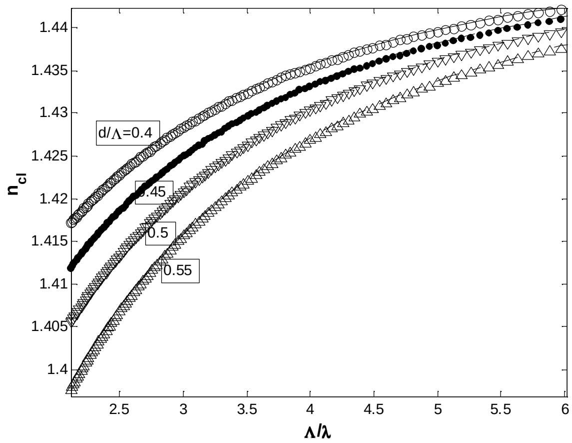

Fig. 2. Comparison of fundamental space filling mode index calculated from different numerical methods: shaped plots – Finite Element Method (FEM), line plots - Beam Propagation Method (BPM).

2. Modal cutoff

In the context of a simple MOF, it is necessary to consider the **V** parameter and **V*** which marks the second-order cutoff. It was concluded that **V***=π is applicable for a MOF structure with constant pitch size [7]. And this result has been numerically clarified and confirmed according to:

$$V_{PCF}(\lambda) = \frac{2\pi\Lambda}{\lambda}[n_c^{\,2}(\lambda) - n_{cl}^{\,2}(\lambda)]^{1/2} \qquad (1)$$

where $n_c(\lambda)=c\beta/\omega$ is the effective index of the fundamental mode, **c** is the speed of light, β is the propagation constant, and ω is the angular frequency. Similarly n_{cl} is the effective index of the fundamental space-filling mode of the unit cell. For our IH-MOF structure, the periodic cross-section of the structure is modified because of the existence of interstitial air holes as shown in Fig. 1(d). And this effective "cladding" index will be smaller than that of the fundamental space-filling mode in a simple triangular lattice without interstitial holes. Definitely, similar influence also exists on the effective index of fundamental mode. However, from the calculation results, we can conclude the influence on n_{cl} is more significant than on n_c. Therefore the Numerical Aperture (NA), (n_c^2- n_{cl}^2), will be larger for our IH-MOF, and we expect an increase of the cutoff wavelength according to equation (1).

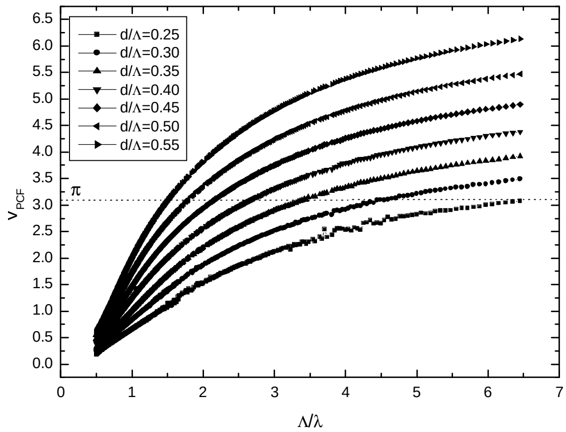

Fig. 3. Numerical results for V parameter with different air-hole diameter (from the bottom, d/Λ=0.3, 0.35, 0.4, 0.45, 0.5, 0.55).

It has been verified that simple triangular latticed MOF structures will be so called "endlessly single mode" when d/Λ<0.4, i.e., single mode over a wide range of wavelengths [1]. In case of IH-MOF, there is an increase of cutoff wavelength, so structures with smaller **d/Λ** size will have the endlessly single mode property. In the fiber stack and drawing process of triangular latticed MOFs, tiny interstitial air regions will unavoidably remain in the fiber cladding after drawing. Since the guiding mechanism is still index guiding, the shape of the air region will not influence the cutoff. Instead, it is the air-filling fraction, which is an important factor to determine NA. We choose the interstitial air hole size that has equivalent area as the gap regions between three identical capillaries, that is $\mathbf{p}_{max}=0.1133\Lambda$. Results of **V** parameters calculated according to Equation (1) for various **d/Λ** are shown in Fig. 3. The single mode operation regime is $\mathbf{V}_{PCF}< \pi$, thus IH-MOF with **d/Λ**<0.25 will be single mode over a wide range of wavelengths. The calculated new cutoff condition provides a more promising guideline for designing an endlessly single mode MOF.

3. Dispersion property

Fiber dispersion plays a critical role in optical communication because different spectral components of an optical pulse have different propagation speed. In MOFs, chromatic dispersion is strongly related to the air-hole structure, which provides a large tunability of dispersion for various applications; therefore, we can expect different dispersion characteristics for the IH-MOFs because of the modification of the air-hole structure. The chromatics dispersion, including waveguide and material dispersions, can be directly calculated from the effective index of the fundamental mode over a range of wavelength [8].

$$D(\lambda) = -\frac{\lambda}{c}\frac{d^2 n_{eff}(\lambda)}{d\lambda^2} \tag{2}$$

This method is proven to be valid for non-completely periodic cladding structures and even for noncircular air holes [9]. When the **d/Λ** ratio is fixed, we calculate the chromatic dispersion from Equation (2). With the increase of the interstitial air-hole size, the zero-dispersion-wavelength is shifted to the shorter wavelength. From the results shown in Fig. 4, a 60 nm shift is achieved when the interstitial hole size is increased from **p**=0 to $\mathbf{p}_{max}$=0.1133Λ. This agrees well with the blue-shift phenomenon in a conventional MOF when we increase the air-filling fraction, because the cladding becomes more dispersive.

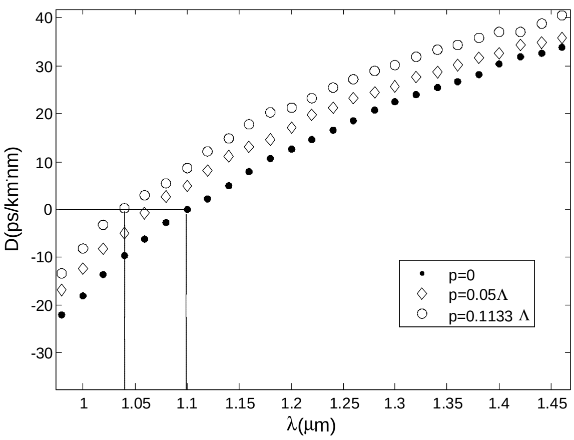

Fig. 4. Chromatic dispersion of IH-MOFs with different interstitial air-hole size, d/Λ=0.3.

4. Confinement loss improvement

Confinement loss is an additional form of loss that occurs in single-material fibers which is determined by the geometry of the waveguide structure [3]. It can be calculated from:

$$L = \frac{20\times10^6}{\ln 10}\frac{2\pi}{\lambda(um)}\mathrm{Im}(n_{eff})dBm \tag{3}$$

We can expect the confinement loss will be reduced significantly by increasing the size of the assistant holes. As shown in Table 1, at **λ**=1.55 μm, **d/Λ**=0.5, number of air-hole rings is 3, the confinement loss for a MOF without interstitial holes is 1.21dB/m. After employing the interstitial holes with diameter 0.1133Λ, the confinement loss is reduced to 0.01dB/m, which is a significant improvement.

*Table 1. Confinement loss for different assistant air-hole size **p**. d=2μm, Λ=4μm, **λ**=1.55μm.*

p	Imaginary (n_{eff})	$Loss_{confinement}$
0	3.448×10^{-8}	1.21dB/m
0.1Λ	1.082×10^{-8}	0.38dB/m
0.105Λ	2.052×10^{-9}	0.07dB/m
0.1133Λ	2.881×10^{-10}	0.01dB/m

It was concluded that the mode is more tightly confined for larger air-filling fractions [3]. However, the confinement in our IH-MOF design is even better than the simple MOF structure with same air-filling fraction. For the structure without interstitial holes, **L**=0.33 dB/m when **d/Λ**=0.525. While for an IH-MOF with the same air-filling fraction (**d/Λ**=0.5, **p**=0.1133Λ), **L**=0.01 dB/m. This is because the effective air-filling fraction of the inner air-hole rings will influence more on the confinement. The interstitial holes effectively block the leakage through those silica bridges. Correspondingly, the effective mode area A_{eff} is calculated with [8]:

$$A_{eff} = \frac{\left(\iint \left|E(x,y)^2\right| dxdy\right)^2}{\iint \left|E(x,y)\right|^4 dxdy} \tag{4}$$

where $E(x,y)$ is the modal distribution for the fundamental mode in the transverse direction. The effective mode area is 20.3286 μm^2 for a conventional MOF (**d**=2 μm, **Λ**=4 μm, **λ**=1.55 μm) without interstitial air holes. Different mode distributions are shown in Fig. 5. Because of the solid capillary of the core, the interstitial holes may not exist in the most inner rings, and it is treated as "partial" IH-MOF. A_{eff} is calculated to be 18.6371 μm^2 in this case. A "full" IH-MOF has interstitial holes in every super cell, such that the even smaller effective area is 12.0725 μm^2. Since the nonlinear coefficient is inversely proportional to A_{eff}, the nonlinear factor will increase by 50% by introducing the interstitial air holes.

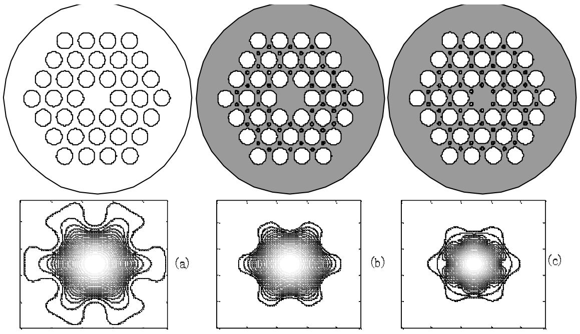

Fig. 5. Fiber cross-sections and effective mode distribution: (a) conventional MOF (b) "partial" IH-MOF (c) "full" IH-MOF.

5. Conclusion

In conclusion, we have theoretically investigated the waveguide characteristics of a novel IH-MOFs structure, including modal cutoff, chromatic dispersion and mode confinement. A more promising guideline for designing an endlessly single mode MOF is obtained, **d/Λ**<0.25, which is smaller than the endlessly single mode operation ratio in a MOF without interstitial holes **d/Λ**<0.4. The zero-dispersion-wavelength is blue-shifted as large as 60 nm with influence of interstitial holes. Also, the leaky loss can be significantly reduced and the nonlinearity will be enhanced by 50% because of tighter confinement. This hole-assistant microstructure can provide direct manipulation of dispersion and nonlinearity properties, thus these novel fibers are ideally suitable for tunable fiber devices in optical communication.

References

[1] T. A. Birks, J. C. Knight, P. S. J. Russell, "Endlessly single mode photonic crystal fibre", Optics Letter, **22**, 961 (1997).
[2] K. Saitoh, M. Koshiba, T. Hasegawa, E. Sasaoka, "Chromatic dispersion control in photonic crystal fibers: application to ultra-flattened dispersion", Optics Express **11**, 843 (2003).
[3] V. Finazzi, T. M. Monro, D. J. Richardson, "Small-core silica holey fibers: nonlinearity and confinement loss trade-offs" J. Opt. Soc. Am. B **20**, 1427 (2003).
[4] T. A. Birks, P. J. Roberts, P. St. J. Russell, "Photonic band gap guidance in optical fibers", Optics Letter, **31**, 1941 (1997).
[5] J. Broeng, S. E. Barkou, A. Bjarklev, J. C. Knight, T. A. Birks, P. St. J. Russell, "Highly increased photonic band gaps in silica/air structures", Optics Communication **156**, 240 (1998).
[6] A. Cucinotta, S. Selleri, L. Vincetti, M. Zoboli, "Holey Fiber Analysis Through the Finite-Element Method", IEEE Photon. Technol. Lett. **14**, 1530 (2002).
[7] N. A. Mortensen, J. R. Folkenberg, M. D. Nielsen, K. P. Hansen, "Modal cutoff and the V parameter in photonic crystal fibers", Optics Letter **28**, 1879 (2003).
[8] G. Agrawal, Nonlinear Fiber Optics. New York: Academic, (1995).
[9] A. Ferrando, E. Silvestre, J. J. Miret, P. Andres, "Nearly zero ultraflattened dispersion in photonic crystal fibers", Optics Letter **25**, 790 (2000).

*Corresponding author: p145144582@ntu.edu.sg